

## Mechanical characterization of millimetric agarose spheres using a resonant technique

J. YESCAS<sup>1</sup>), P. MANDAL<sup>1</sup>), J. SINHA<sup>1</sup>), R. SNOOK<sup>2</sup>), J. HAWKES<sup>2</sup>),  
P. MORENO GARIBALDI<sup>3</sup>), R. CARRERA-ESPINOZA<sup>3</sup>)

<sup>1</sup>) *Department of Mechanical Aerospace and Civil Engineering, The University of Manchester, M139PL UK, e-mail: jayescash@hotmail.com*

<sup>2</sup>) *Manchester Institute of Biotechnology, The University of Manchester, Princess St, Manchester, M1 7DN, UK*

<sup>3</sup>) *University of the Americas (UDLAP), San Andrés Cholula, Puebla, Mexico*

THIS PAPER PRESENTS A METHODOLOGY for the mechanical characterization of agarose millimetric spheres using resonant principles. Detection of the modes of vibration was conducted using a low-cost experimental setup based on an electret microphone adapted with a thin latex elastic membrane for the sensing stage and a piezoelectric actuator driven by a conventional transformer for the excitation stage. The identification of vibration modes is supported through an ANSYS Finite Element model of the experimental setup. Experimental and numerical results demonstrate that two modes of vibration, known as Quadrupole and Octupole, appear in the amplitude spectrum and can be used to obtain stiffness values for the samples. Following this approach, Young's modulus of  $209 \pm 19.80$ ,  $338 \pm 35.30$  and  $646 \pm 109$  kPa for 2%, 3% and 4% agarose millimetric spheres were calculated.

**Key words:** agarose spheres, resonance experiment, bulk mechanical properties, tissue engineering, Young's modulus, 3D scaffolds.

Copyright © 2020 by IPPT PAN, Warszawa

### Notation

$\xi$	spheroidal normalised frequency,
$\eta$	torsional normalised frequency,
$j$	spherical Bessel function of the second type,
$\nu$	Poisson's ratio,
$k$	system stiffness,
$k_m$	membrane stiffness,
$i f_0$	experimentally obtained spheroidal modes of vibration,
$E$	Young's modulus,
$a$	sphere radius,
$\rho$	sphere density,
PZT	Lead Zirconate Titanate based piezoelectric material,
$\sigma$	equibiaxial stress,
$t_0$	membrane initial thickness,
$C_0$	initial reference length,
$C$	bubbles arc length,

$P$	inflation pressure,
$r$	radius of curvature,
$\delta$	membrane deflection,
R1–R3	1st, 2nd and 3rd peaks of resonance appearing in the amplitude spectra experimentally,
$E_{OP}$	Young’s modulus of elasticity calculated using the Octupole mode of vibration,
AFM	Atomic Force Microscope,
$m_{sample}$	mass of the spherical sample.

## 1. Introduction

THE STIFFNESS OF MILLIMETRE AND CENTIMETRE SIZED BODIES is an important parameter of study in tissue engineering for the construction of hydrogel-based scaffolds and in cancer research for the mechanical characterization of tumours removed from patients. In tissue engineering, it is known that the stiffness of gel-based scaffolds influences parameters of the cell culture such as locomotion, growth, differentiation and proliferation [1–3]. In cancer research, new tools for the early detection of cancer, based on the indirect measurement of the stiffness of spherical masses inside the human body have been recently proposed [4]. In both cases, materials are known to behave viscoelastically, and for this reason, their full quantitative mechanical characterization requires either excessive manipulation or even destruction of the sample, for example when carrying out a rheological test, thus, eliminating the possibility of monitoring the stiffness evolution during specific experiments such as cell culture or tumour development.

An alternative to assess the stiffness of viscoelastic materials is by assuming small deformations and therefore a purely elastic behaviour. This assumption has been widely accepted in cell mechanics, for example when testing biological cells using the indentation test carried out in the Atomic Force Microscope (AFM) [5], in which, researchers are able to represent the stiffness of complex systems with a reduced number of variables named equivalent Young’s modulus and Poisson’s ratio. In addition, knowing that resonances of linear elastic bodies depend only on their geometry, mass and stiffness properties, the mechanical characterization of samples of known geometry and density using a methodology based on a vibration test is possible.

Some of the main advantages of carrying out a vibration test include minimal deformation of the sample during the test, non-destructive nature of the characterization as well as the possibility to adapt the testing setup in other experiments, for example in bioreactors flasks for tissue engineering. This test is well known, and has been in use for example in the food industry for the classification of fruit and vegetables [6–7], and in the materials science industry for the mechanical characterization of materials [8, 9].

This paper explores the possible use of a vibration test to carry out a non-destructive mechanical characterization of soft bodies in the millimetre range.

Since the study of vibrations of finite bodies made of soft materials is not as common as the study of hard materials, this paper is preliminary research carried out on spheres of millimetric size made of agarose. Moreover, in order to reduce the number of variables involved, the experiments were carried out in air instead of a liquid environment, and the identification of modes of vibration was supported both theoretically and through a Finite Element (FE) study.

### 2. Vibrations of an elastic sphere

The problem of finding the resonant frequencies of an ideal elastic sphere was first solved by LAMB [10]. He found that the solution of the problem only depends on sphere diameter, density, shear modulus and Poisson’s ratio. Lamb classified the resonant frequencies in two categories, named torsional and spheroidal. The torsional modes are characterised by displacements occurring only in the theta and phi directions (in a spherical coordinates system) and by their independence with the Poisson’s ratio value. On the other hand, spheroidal modes are characterized by displacements in all directions. As previously reported by ERINGEN [11] and SAVIOT [12], the resonances of an elastic sphere are conveniently expressed as normalised frequencies for the spheroidal ( $\xi$ ) and torsional ( $\eta$ ) modes whose values correspond to the roots of Eq. (2.1), given by:

$$(2.1) \quad \begin{vmatrix} \left(l^2 - l - \frac{\eta^2}{2}\right) j_{l+0.5}(\xi) + 2\xi j_{l+1.5}(\xi) & l(l+1)[(l-1)j_{l+0.5}(\eta) - \eta j_{l+1.5}(\eta)] \\ (l-1)j_{l+0.5}(\xi) - \xi j_{l+1.5}(\xi) & \left(l^2 - 1 - \frac{\eta^2}{2}\right) j_{l+0.5}(\eta) + \eta j_{l+1.5}(\eta) \end{vmatrix} = 0$$

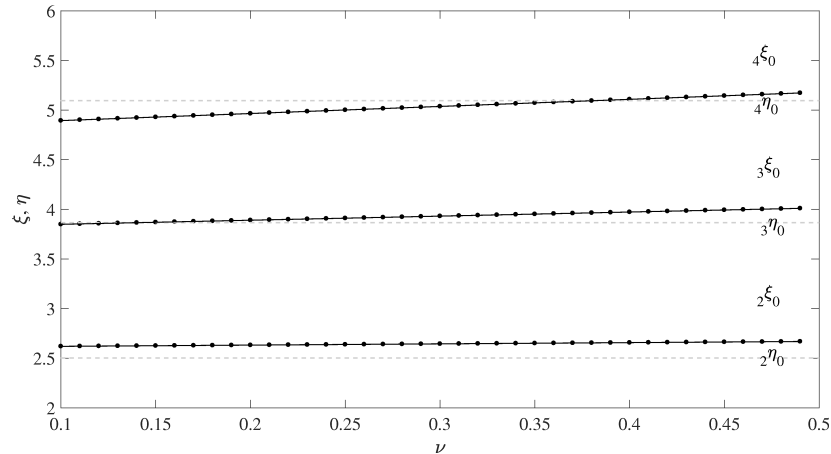


FIG. 1. Normalized torsional and spheroidal frequencies. Notice that torsional modes (grey dashed lines) do not depend on Poisson’s ratio and spheroidal modes behave in a linear fashion. Continuous lines correspond to the fitted functions of the roots of Eq. 2.1 (dots).

where  $j$  represents the spherical Bessel functions of the second type, which can be solved for different values of  $l$  by assuming that the material is isotropic ( $\frac{\eta}{\xi} = \sqrt{\frac{1-2\nu}{2-2\nu}}$ ). The behaviour of the lowest normalised modes ( $l = 2, 3, 4$ ) are shown in Fig. 1.

In this work, the lowest spheroidal modes are fitted to a straight line using the least square technique. In this way, normalized frequencies can be obtained as a function of Poisson's ratio ( $\nu$ ) through:

$$(2.2) \quad {}_l\xi_0 = m_l\nu + b_l$$

values fitted for  $l = 2, 3$  and 4 are summarized in Table 1.

**Table 1. Fitting constants for the lowest spheroidal modes of vibration.**

$l$	$m_l$	$b_l$
2	0.12	2.6
3	0.41	3.8
4	0.71	4.82

From Fig. 1, Eq. (2.2), and Table 1 it is clear that, theoretically, the ratio between two spheroidal frequencies is only a function of Poisson's ratio for example, for  $l = 2$  and  $l = 3$ , this ratio is given by:

$$(2.3) \quad \frac{{}_3f_0}{{}_2f_0} = \frac{0.41\nu + 3.80}{0.12\nu + 2.60}$$

where  ${}_3f_0$  and  ${}_2f_0$  are the experimentally obtained and properly identified spheroidal modes of vibration. Additionally, a normalised frequency can be calculated using Eq. (2.2) in order to estimate a value for the Young's modulus ( $E$ ) of a spherical sample through [6, 13]:

$$(2.4) \quad f_S = \frac{{}_l\xi_0}{2\pi a} \sqrt{\frac{E(1-\nu)}{\rho(1+\nu)}}$$

where  $a$  and  $\rho$  are the sphere radius, and density respectively. Assuming that the material is purely elastic, Shear modulus ( $G$ ) is calculated using:

$$(2.5) \quad G = \frac{E}{2(1+\nu)}.$$

### 3. Experimental setup and procedure

#### 3.1. Components

The procedure to test spherical samples begins with the computer that controls a signal generator (TGP3122) to produce a sweep of 5 V sine signals ranging from 0.1 to 10 kHz, the voltage is then amplified using a conventional 6–250 V

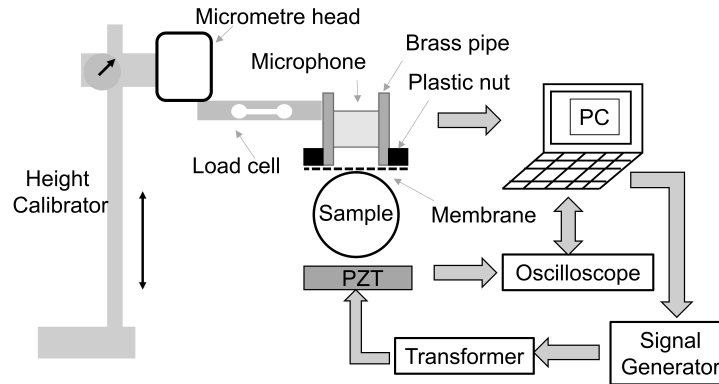


FIG. 2. Experimental setup for testing soft samples.

transformer and fed to a  $11 \times 10 \times 3$  mm Lead Zirconate Titanate based piezoelectric material (PZT, PZ26, Meggit). The sample is excited by the PZT and the motion sensed by a vibration sensor formed by a conventional electret microphone adapted with a latex membrane and a tube forming an air filled closed cavity. Audio is recorded using a Matlab subroutine and the sound card available in the laptop (Conexant Smart Audio HD V 8.54.0.53). The membrane-sample contact was controlled manually with a height calibrator for coarse motion (Mitutoyo 570-312) and digital micrometre head for fine motion (Mitutoyo 164-101). Measuring of the compression force was accomplished through a load cell (accuracy 0.01 mN).

### 3.2. Testing procedure

At the beginning of each test, the sample is placed on top of the PZT plate, and the vibration sensor is carefully brought in contact with the upper region of the sphere up to a force of  $5 \pm 0.50$  mN. Motion from the PZT propagates through the sample and reaches the vibration sensor, so that, small displacements at the sphere pole move the membrane generating a sound pressure recorded by the microphone at a sampling rate of 96 kHz. The signal was converted to amplitude spectrum using the Fourier transform. Additionally, after testing of each group of spheres, the sample is substituted for a 4 mm steel sphere in order to determine the membrane stiffness for displacements ranging from 0.01–0.5 mm.

## 4. Samples and membranes preparation

### 4.1. Agarose spheres

Spherical gel samples were prepared by mixing separately 0.2, 0.3, and 0.4 g of agarose powder (Sigma Aldrich) with 10 ml of hot water ( $70^\circ$  [14]) to obtain

2%, 3% and 4% concentrations. The suspensions were stirred for 15 minutes and placed in an oven at 90° for three hours in order to obtain a homogeneous solution which was poured into a heated glass burette adapted with disposable pipette tips of different diameter to obtain different sphere sizes. By controlling the temperature and opening of the burette tap, drops of suspension of approximately 3–6 mm in diameter were gently released on the surface of automotive oil (SAE 5W30) contained in a cooled glass tube (6°C) of 80 cm in height. Once the drop came into contact with the oil, it naturally acquired a spherical shape which was kept as it was cooling and settling down by gravity towards the base of the cylinder. The spheres deposited on the bottom were separated and rinsed using a strainer and soapy water.

#### 4.2. Membrane preparation

Membrane stretching was carried out using the bubble inflation biaxial test [15] following the procedure described by DREXLER [16]. Here, pressure coming from a water column is used to inflate a circular latex blank ( $\phi$  32 mm) up to a height of 16 mm to form a semi-sphere, then at least four aluminium nuts ( $\phi$  8 mm) were carefully glued to the bubble surface to obtain a membrane-nut element. Stress level was estimated using the Young-Laplace equation for inflation of spheres [15, 16]:

$$(4.1) \quad \sigma \frac{C_0^2 t_0}{C^2} = \frac{Pr}{2}$$

where  $\sigma$  is the equibiaxial stress,  $t_0$  is the membrane initial thickness ( $70 \pm 20 \mu\text{m}$ ),  $C_0$  is the initial reference length (32 mm) and  $C$  is the bubbles arc length,  $P$  is the inflation pressure, and  $r$  is the radius of curvature. Experimental data was then fitted using the strain energy function

$$(4.2) \quad \sigma = \mu (\lambda^2 - \lambda^{-4})$$

where  $\lambda = \frac{C}{C_0}$  is the biaxial stretch. Fitted variables with this function produce values for  $\mu = 435 \pm 35 \text{ kPa}$ , which are similar to those reported previously [16].

To determine the membrane flexural stiffness, 16 nut-membrane elements were pressed against a 4 mm rigid sphere, and the force-displacement measurements were fit to a second-order polynomial equation (see Fig. 3). The first derivative of the fitting function was used to calculate an equivalent stiffness value for the membrane ( $k_m$ ). Using this procedure the stiffness of the membranes used for this work was determined to be  $k_m = 83.68 \pm 5.30 \text{ mN/mm}$ . This value corresponds to a 10 mN force which causes a deflection ( $\delta$ ) value of 0.10 mm.

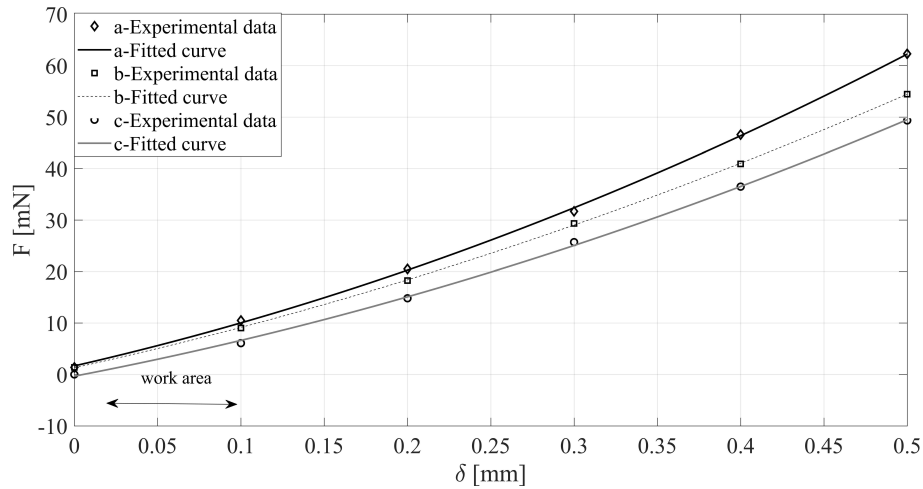


FIG. 3. Fitted curves (continuous lines) of the experimental force-indentation data ( $\diamond$ ,  $\square$  and  $\circ$  markers) of 3 representative membranes (a, b, and c).

## 5. Experimental results

### 5.1. Vibration test

The recorded spectra for sweep excitation showed at least three clear peaks of resonance (R1, R2, and R3 in Fig. 4) and in most cases fourth peak (R4 in Fig. 4). For all agarose concentrations (2%, 3%, and 4%), peak R1 is a sharp peak with the highest amplitude that consistently remains in the interval ranging from 500 to 1200 Hz, also, peak R2 is higher when compared to R3.

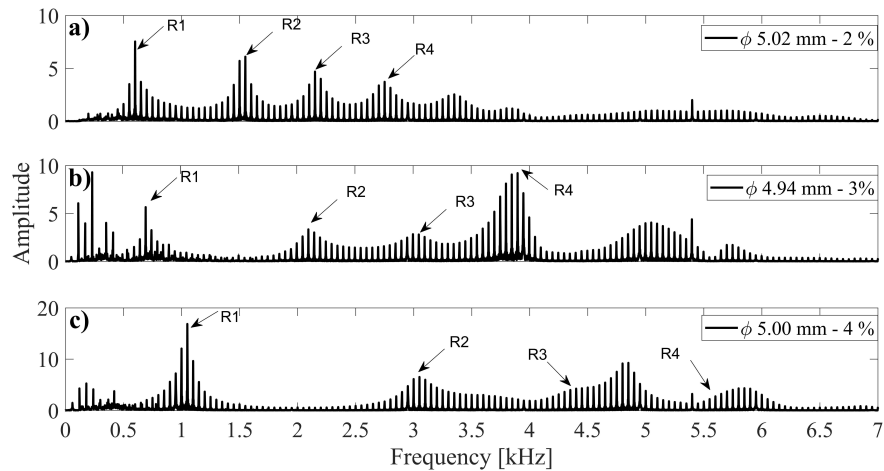


FIG. 4. Typical amplitude spectra of samples of similar size ( $\phi$  5 mm) and different agarose composition.

### 5.2. Effect of compression force

It is known that external forces could influence the resonant behaviour of vibrating systems and for this reason when carrying out Resonant Ultrasound Spectroscopy experiments on hard samples [17], they are gently pressed against two flat surfaces so that the force is assumed to be small enough not to modify the resonant behaviour of the sample under test. However, since samples studied in this work are soft, even a small force could cause them to behave viscoelastically and consequently modify their resonance properties. Therefore, to determine the effect of force on the resonant frequencies, two groups (2% and 4% agarose) of four samples of approximately 3.9 mm in diameter were tested at different compression forces. It is clear from Fig. 5 that the R1 and R2 peaks shift towards higher frequencies as the force increases and the position of peak R3 does not show a significant dependence at least for forces under 10 mN for both 2% and 4% agarose. Maximum standard deviations were 3% for R1, 4% for R2 and 8% for R3.

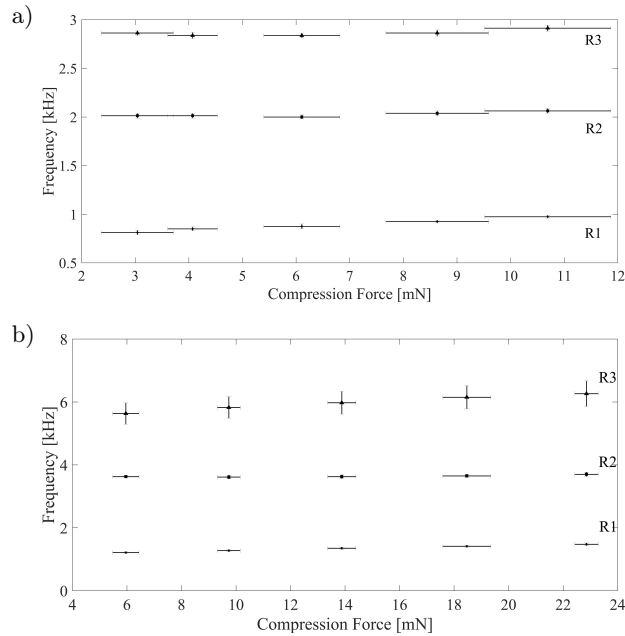


FIG. 5. Shift of resonances as a function of the initial compression force for a set of four spheres of a)  $\phi_{avg} = 3.81 \pm 0.07$  mm and 2% agarose concentration and b)  $\phi_{avg} = 3.9 \pm 0.08$  mm and 4% agarose concentration.

### 5.3. Effect of membrane selection

To prove that the membrane was properly stretched, a group of three nut-membranes was used to measure the resonant frequencies of four samples (4, 4.73,

4.87 and 5.52 mm). These nut-membranes were obtained from the same stretched latex sheet but different blanks. Figure 6 reveals that there is little variation in the resonant frequencies measured. For all experiments, the standard deviation remains under 8% of the average frequency.

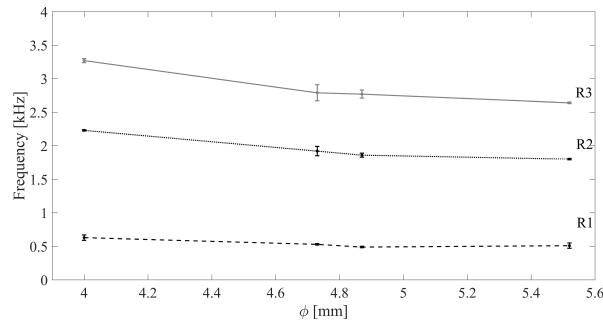


FIG. 6. Resonant frequencies of 4 samples made of 3% agarose, measurements were made using three membranes. The compression force was set to 10 mN.

#### 5.4. Effect of sphere size

Sphere diameter is the variable that showed the biggest influence on the behaviour of the samples. In Fig. 7, it is possible to observe a decreasing value in resonant frequencies for R1, R2 and R3 as the sample size increases. Although sometimes smaller samples have lower frequencies compared to samples of similar size, this downshift is observed in all three frequencies, thus indicating a possible uncertainty in the size measurement, this phenomenon is signalled using black arrows in Fig. 7.

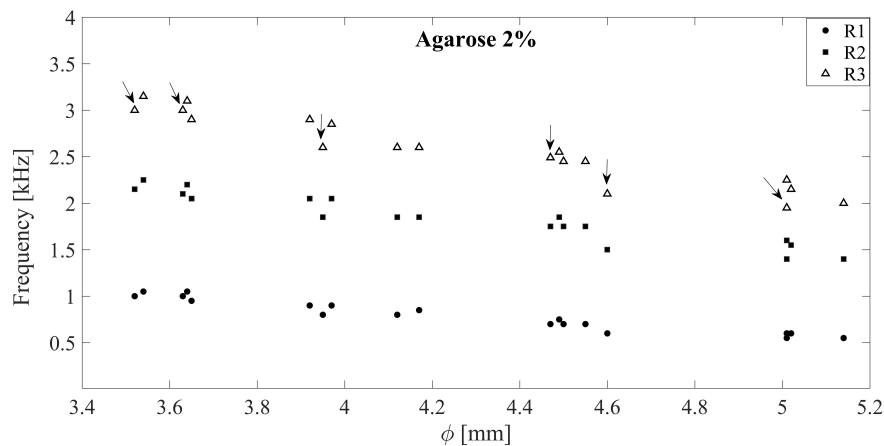


FIG. 7. Resonant frequencies for samples made of 2% agarose. Compression force was set to 10 mN.

### 5.5. Numerical model

ANSYS was used to construct a FE model of the vibration test, as Fig. 8 shows, it consists of a sphere connected to a pair of springs at its poles representing the whole system stiffness. In this model, two surfaces located at  $25\ \mu\text{m}$  above the bottom and below the top of the sphere poles were created in order to restrict the motion only in the vertical direction (BC1 and BC2) and to connect the springs. The sample was modelled using a solid sphere made of SOLI186 elements with an average size of 5% of the sphere diameter. The density value ( $972 \pm 28\ \text{kg/m}^3$ ) was obtained by measuring the samples weight and diameter using an analytic scale (METTLER PM600) and a micrometre gauge. A general damping value of 0.1 was set in order to account for the damping of the sample and medium, this value was estimated using the half-power bandwidth rule and the amplitude spectra of experimental data.

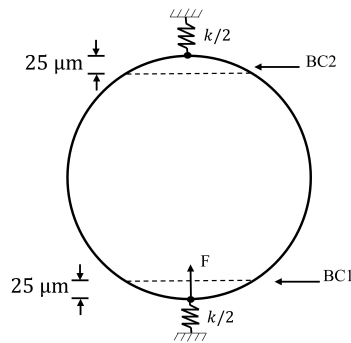


FIG. 8. Diagram used to construct the FE model of the vibration test.

Two types of analysis were mainly carried out: modal analysis and harmonic analysis. The first simulation is aimed to determine the effect of spring stiffness on the position of resonances and the second analysis is aimed to obtain the amplitude spectra when a vertical excitation is used ( $F = 5\ \text{mN}$ ) and in this way reveal the origin of the resonances. In general simulations are carried out using a compression force of 5 mN, Young's modulus in the interval  $100 < E < 646\ \text{kPa}$ , a sphere diameter  $3 < \phi < 6\ \text{mm}$ , and a springs constant between  $0.1 < k < 0.5\ \text{N/mm}$ .

Although Hertz theory can be used for the calculation of the spring constants that represent the contact between PZT-sphere and Sphere Membrane, the mathematical models require variables that are unknown (at the beginning of the test) like  $E$ , and  $\nu$  for the sphere, as well as the force to determine the slope of the force displacement curve. For this reason, the whole system stiffness was calculated using the FE results.

### 5.6. Ratio between R3 and R2

From Eq. 2.3, it is clear that the ratio between R3 and R2 is only a function of Poisson's Ratio (for most materials,  $0 < \nu < 0.5$ ), consequently this ratio should be in the interval  $1.462 < {}_3f_0/{}_2f_0 < 1.504$ . Since experimental data gave smaller values than 1.46, a FE study was conducted in order to explore the possible effect of the system stiffness on this ratio. Numerical results suggest that the ratio decreases as the spring constant increases, following an exponential rule given by:

$$(5.1) \quad \frac{{}_3f_0}{{}_2f_0} = 0.1222e^{-4.71k} + 1.374.$$

This equation describes well both experimental and numerical results as Fig. 9 shows.

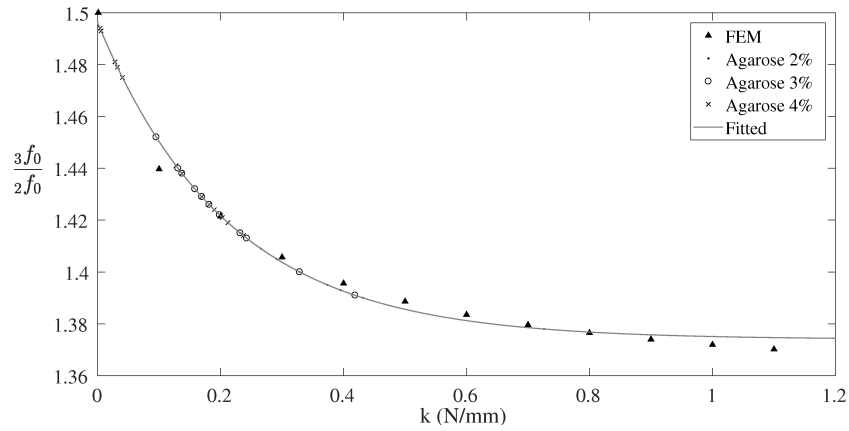


FIG. 9. Ratio  ${}_3f_0/{}_2f_0$  obtained numerically, theoretically, and experimentally.

### 5.7. Determination of Young's modulus

Experimental resonant frequencies obtained for samples made of the same agarose composition depend on both the size and the compression force. Among the resonances, the less immune to compression is R3, since the samples are made of gel ( $\nu \approx 0.5$ ).

In the literature, the first peak is not normally taken into account when carrying out the mechanical characterization of hard samples (see for example [17]) and its origin has not been conclusively determined. It is also known that the spheroidal mode with the lowest frequency is the Quadrupole (identified as  ${}_2\xi_0$ ) and right after is the Octupole (identified as  ${}_3\xi_0$ ). Hence, a first identification for the modes of vibration is that R2 belongs to the Quadrupole and R3 belongs to the Octupole. Therefore, using the information from Table 1

( $m_3 = 0.41$ ,  $b_3 = 3.8$ ) and Eq. (2.4), the normalized frequency is  ${}_3\xi_0 = 4$ , in this way, a Young's modulus value based on the information from the Octupole is given by:

$$(5.2) \quad E_{OP} = 1.5\rho(f_s\pi d)^2.$$

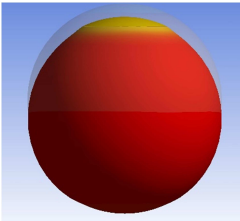
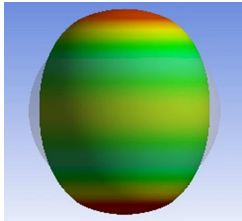
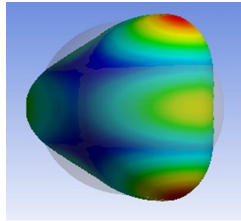
Using Eq. (5.2) Young's modulus for agarose gels of different concentration is estimated as Table 2 summarizes.

**Table 2. Young's modulus for 2%, 3% and 4% agarose spheres.**

Agarose	2%	3%	4%
$E_{OP}$ (kPa)	$209 \pm 19.8$	$338 \pm 35.3$	$646 \pm 109$

A modal analysis was carried out for samples of 4 mm using Young's modulus values shown in Table 2. The deformation and resonances obtained in three ways experimental, numerical and theoretical agree well as Table 3 shows. Notice that the numerical calculation agrees well with the theoretical prediction when there is no spring.

**Table 3. First vertical modes of vibration obtained from a modal analysis simulation. The sample is a 4 mm, 2% agarose sphere, for this simulation  $E = 232$  kPa (\* when the stiffness of spring is zero the value of the QP obtained numerically is 1.88).**

Mode shape			
Experimental	0.9	2.05	2.85
Numerical	0.87	2.1*	2.84
Theoretical	–	1.88	2.84

### 5.8. Origin of R1, R2 and R3

After matching peaks with the deformations shapes in the FEM, it was possible to determine that R1 corresponds to the rigid body motion caused by the mass of the sphere and springs representing contacts (see Table 3a) and the whole system stiffness; R2 corresponds to the Quadrupole deformation (see

Table 3b) and R3 correspond to the Octupole deformation (see Table 3c). Additionally, R1 can be calculated using a lumped model and the stiffness values of the springs as follows:

$$(5.3) \quad R1 = \frac{1}{2\pi} \sqrt{\frac{k_{system}}{m_{sample}}}.$$

## 6. Discussion

The experimental setup presented in this paper proved to be useful to detect at least three peaks of resonance. FEM model suggests that peaks R2 and R3 are spheroidal and belong to the well-known Quadrupole and Octupole modes of vibration. Previous experimental research also supports the idea that our experimental setup preferentially excites spheroidal modes, just like FRAISER [18] preferentially excited torsional modes using a shear actuator.

As stated in the introduction, a mechanical characterization of the samples (i.e. determination of Young's modulus and Poisson's ratio) is possible through vibrations theory, as long as we know the mass and geometric properties. Experimental work showed that agarose spheres have similar density values ( $972 \pm 28$  kg/cm<sup>3</sup>) because their main component is water, also, geometric properties for the samples are fully determined through the diameter, which can be measured with a 10  $\mu$ m accuracy. By assuming that the gels are incompressible ( $\nu = 0.5$ ), the only remaining variable to represent the elastic properties would be Young's modulus. For this reason, experimental and numerical data were focused on finding how this modulus was related to the resonances and to what extent the theory for free vibrations of elastic spheres could be used.

Although experimental and numerical results confirmed that resonances have a marked dependence on the sphere size (see Fig. 7), theoretical predictions for resonances did not seem to represent the experimental setup since the ratio between the Octupole and Quadrupole frequencies gave values outside the interval predicted theoretically ( $1.462 < 3f_0/2f_0 < 1.504$ ) for the whole range of Poisson's ratio ( $0 < \nu < 0.5$ ). For this reason, it was concluded that the measuring system was affecting the vibrating behaviour of the samples. Numerical and experimental data suggest that compression force and system stiffness are the two variables that mainly affect the R3/R2 ratio (see Figs. 5 and 9). These variables are related, because, compression force determines the partial stiffness at the bottom ( $k$  in Fig. 8) of the sphere as the Hertz contact theory states, and also determines the stiffness at the top because it includes the membrane stiffness ( $k_m$ , see Fig.3). By setting the compression to 5 mN, we were able to conduct a parametric numerical study that evidences an exponential dependence between  $3f_0/2f_0$  and  $k$  whose behaviour highly resembles the equation that models the

stress strain relationship in the bubble inflation test (see Fig. 9), thus suggesting that membrane stiffness plays a key role in determining the position of R1 and R2.

Numerical results show that the position of peak R3 has less dependence on the system stiffness, for this reason, the authors propose this frequency to calculate an initial value for Young's modulus of the samples ( $E_{OP}$ ). The  $E_{OP}$  values obtained in this way remained in the interval ranging from 100–650 kPa as observed for 2%, 3%, and 4% agarose spherical samples. These values are in good agreement with previous studies using tests based on contact mechanics principles and rheological techniques [19–23], which situate Young's modulus in the interval ranging from 1 kPa to 1 MPa for an agarose concentration between 1 and 10%. Using an  $E_{OP}$  value in this interval allowed to carry out a parametric study to determine the relationship between the ratio R3/R2 and the system stiffness  $k$ . The results show that there is an exponential dependence between these two variables, and, the mathematical model obtained (see Eq. (5.1) and Fig. 9) accurately describes experimental data.

Elastic properties of millimetric spherical bodies were calculated with the procedure proposed in this paper. It is clear that these properties of agarose can be easily tuned, contrary to rigid bodies where Young's modulus remains within a narrow magnitude for similar alloys, for example, ferrous alloys have almost the same 200 GPa Young's modulus, while a change in one percent of agarose composition could lead to a two-fold difference in the same variable. This is important in tissue engineering for successful 3D cell growing, especially if multiple stiffnesses are to be used [24–26]. These scaffolds could help to construct more complex structures that better mimic real organs like tendons-bone interface tissue [27].

At the moment, the technique used to manufacture the samples only allowed us to obtain agarose spheres closely distributed in size (3–5 mm) whose peaks of resonance are expected to reach 7 kHz for agarose concentration greater than 4%. For this reason, the experimental study presented in this paper was only conducted on samples made of low agarose concentration in order to avoid the overlapping of the resonances of the samples with those of the experimental setup appearing from 7 kHz onwards.

Although there is plenty of information related to the characterization of the stiffness properties of soft materials used for cell culture purposes [28], these techniques are mainly dedicated to carry out the characterization at the beginning and after the culture. To date, very little work has been proposed to estimate the stiffness of the scaffold whilst tissue is being grown [22, 23, 28] and it is only when engineered tissues have already been implanted that monitoring of their stiffness has been carried out using techniques like Magnetic Resonance Imaging [29, 30]. Monitoring of the scaffold stiffness is important because the scaffold

materials are expected to degrade along with time, and significant changes in the stiffness of the engineered tissue might result in insufficient cell proliferation in the engineered part, or in the worst scenario, rejection from the implantation site due to stiffness mismatch between the engineered tissue and the host body [31].

## 7. Conclusion

The experimental setup and methodology proposed in this paper to estimate the stiffness properties of soft materials were proved on millimetric spheres made of agarose. This setup proved to be useful for the obtaining of an amplitude spectra of the sample in which, two widely known peaks of resonance Quadrupole and Octupole modes of vibration were identified and corroborated through a numerical simulation. Since the ratio between R3 and R2 could not be described in terms of the equation of motion for a free sphere, a mathematical model to determine the whole system stiffness was proposed. By using the frequency of the Octupole mode of vibration, equivalent Young's moduli of  $209 \pm 19.80$  kPa,  $338 \pm 35.30$  kPa, and  $646 \pm 109$  kPa were calculated for 2%, 3% and 4% agarose gels. This study could contribute to the finding of resonances of micrometric spheres such as suspended biological cells whose existence remains as an open question, and that can be investigated using techniques such as AFM that highly resemble the experimental setup presented in this paper.

## References

1. N.D. LEIPZIG, M.S. SHOICHET, *The effect of substrate stiffness on adult neural stem cell behavior*, *Biomaterials*, **30**, 36, 6867–6878, 2009.
2. N.L. HALLIDAY, J.J. TOMASEK, *Mechanical properties of the extracellular matrix influence fibronectin fibril assembly in vitro*, *Experimental Cell Research*, **217**, 1, 109–117, 1995.
3. R.J. PELHAM, Y. WANG, *Cell locomotion and focal adhesions are regulated by substrate flexibility*, *Proceeding of the National Academy of Sciences*, **94**, 25, 136610–13665, 1997.
4. A.H. HENNI, C. SCHMITT, I. TROP, G. CLOUTIER, *Shear wave induced resonance elastography of spherical masses with polarized torsional waves*, *Applied Physics Letters*, **100**, 13, 1337021–1337025, 2012.
5. J. DOMKE, M. RADMACHER, *Measuring the elastic properties of thin polymer films with the atomic force microscope*, *Langmuir*, **14**, 12, 3320–3325, 1998.
6. E. KIMMEL, K. PELEG, S. HINGA, *Vibration modes of spheroidal fruits*, *Journal of Agricultural Engineering Research*, **52**, 201–213, 1992.
7. E. MACRELLI, A. ROMANI, R.P. PAGANELLI, E. SANGIORGI, M. TARTAGNI, *Piezoelectric transducers for real-time evaluation of fruit firmness. Part II: Statistical and sorting analysis*, *Sensors Actuators A Physical*, **201**, 497–503, 2013.

8. G. RAJESHKUMAR, V. HARIHARAN, *Free vibration characteristics of phoenix Sp fiber reinforced polymer matrix composite beams*, Procedia Engineering, **97**, 687–693, 2014.
9. M. THOMASOVÁ, P. SEDLÁK, H. SEINER, M. JANOVSKÁ, *Young's moduli of sputter-deposited NiTi films determined by resonant ultrasound spectroscopy: Austenite, R-phase, and martensite*, Scripta Materialia, **101**, 24–27, 2015.
10. L. HORACE, *On the vibrations of an elastic sphere*, Proceedings of the London Mathematical Society, **1-13**, 1, 189–212, 1881.
11. A.C. ERINGEN, E.S. SUHUBI, *Elastodynamics, Vol. 2: Linear Theory*, Academic Press Inc., New York, 1975.
12. L. SAVIOT, D.B. MURRAY, *Longitudinal versus transverse spheroidal vibrational modes of an elastic sphere*, Physical Review B: Condensed Matter and Materials Physics, **72**, 20, 1–6, 2005.
13. A. YAOITA, T. ADACHI, A. YAMAJI, *Determination of elastic moduli for a spherical specimen by resonant ultrasound spectroscopy*, Non Destructive Testing International, **38**, 7, 554–560, 2005.
14. Q. CHEN, B. SUKI, K.-N. AN, *Dynamic mechanical properties of agarose gels modeled by a fractional derivative model*, Journal of Biomechanical Engineering, **126**, 5, 666–671, 2004.
15. D.D. JOYE, G.W. POEHLEIN, C.D. DENSON, *A bubble inflation technique for the measurement of viscoelastic properties in equal biaxial extensional flow*, Transactions of the Society of Rheology **16**, 3, 421–445, 1972.
16. E.S. DREXLER, A.J. SLIFKA, J.E. WRIGHT, C.N. MCCOWAN, D.S. FINCH, T.P. QUINN, *An experimental method for measuring mechanical properties of rat pulmonary arteries verified with latex*, Journal of Research of the National Institute of Standard and Technology, **108**, 3, 183–191, 2003.
17. A. MIGLIORI, J.L. SARRAO, W.M. VISSCHER, T.M. BELL, M. LEI, Z. FISK, R.G. LEISURE, *Resonant ultrasound spectroscopic techniques for measurement of the elastic moduli of solids*, Physical Review B: Condensed Matter and Materials Physics, **183**, 1-2, 1–24, 1993.
18. D.B. FRASER, R.C. LE CRAW, *Novel method of measuring elastic and anelastic properties of solids*, Review of Scientific Instruments, **35**, 9, 1113–1115, 1964.
19. Y. MU, A. LYDDIATT, A.W. PACEK, *Manufacture by water/oil emulsification of porous agarose beads: effect of processing conditions on mean particle size, size distribution and mechanical properties*, Chemical Engineering and Processing: Process Intensification, **44**, 10, 1157–1166, 2005.
20. R. MERCADÉ-PRIETO, Z. ZHANG, *Mechanical characterization of microspheres capsules, cells and beads: a review*, Journal of Microencapsulation, **29**, 3, 277–285, 2012.
21. Y. YAN, Z. ZHANG, J.R. STOKES, Q.Z. ZHOU, G.H. MA, M.J. ADAMS, *Mechanical characterization of agarose micro-particles with a narrow size distribution*, Powder Technology, **192**, 1, 122–130, 2009.
22. J. RAUH, F. MILAN, K.-P. GÜNTHER, M. STIEHLER, *Bioreactor systems for bone tissue engineering*, Tissue Engineering Part B Review, **17**, 4, 263–280, 2011.

23. A.B. YEATTS, J.P. FISHER, *Bone tissue engineering bioreactors: Dynamic culture and the influence of shear stress*, *Bone*, **48**, 2, 171–181, 2011.
24. A. BIRGERSDOTTER, R. SANDBERG, I. ERNBERG, *Gene expression perturbation in vitro – A growing case for three-dimensional (3D) culture systems*, *Seminars in Cancer Biology*, Special Issue, **15**, 5, 405–412, 2005.
25. B.A. JUSTICE, N.A. BADR, R.A. FELDER, *3D cell culture opens new dimensions in cell-based assays*, *Drug Discovery Today*, **14**, 1–2, 102–107, 2009.
26. M.E. BREGENZER, E.N. HORST, P. MEHTA, C.M. NOVAK, T. REPETTO, C.S. SNYDER, G. MEHTA, *Tumor modeling maintains diverse pathology in vitro*, *Annals of Translational Medicine*, **7**, S8, S262–S262, 2019.
27. Y. CAO, S. YANG, D. ZHAO, Y. LI, *Three-dimensional printed multiphase scaffolds with stratified cell-laden gelatin methacrylate hydrogels for biomimetic tendon-to-bone interface engineering*, *Journal of Orthopaedic Translation*, **23**, 2020.
28. Z.-Y. ZHANG S.H. TEOH, E.V. TEO, M.S.K. CHONG, C.W. SHIN, F.T. TIEN, M.A. CHOLANI, J.K.Y. CHAN, *A comparison of bioreactors for culture of fetal mesenchymal stem cells for bone tissue engineering*, *Biomaterials*, **31**, 33, 8684–8695, 2010.
29. J.M. WALKER, A.M. MYERS, M. SCHLUCHTER, V.M. GOLDBERG, *Nondestructive evaluation of hydrogel mechanical properties using ultrasound*, *Annals of Biomedical Engineering*, **39**, 10, 2521–2539, 2011.
30. H. XU, S.F. OTHMAN, R.L. MAGIN, *Monitoring tissue engineering using magnetic resonance imaging*, *Journal of Bioscience and Bioengineering*, **106**, 6, 515–527, 2008.
31. S. WU, X. LIU, K. W.K. YEUNG, C. LIU, X. YANG, *Biomimetic porous scaffolds for bone tissue engineering*, *Materials Science & Engineering R: Reports*, **80**, 1–36, 2014.

Received March 10, 2020; revised version June 2, 2020.

Published online June 30, 2020.

---

